Table 2 Number of reads and read depth of each sample

Sample	HBV-P10140	HBV-P10193	HBV-P10234	HBV-P10264	HBV-P11021	HBV-P12009
No. of reads mapping on HBV reference	187 336	186 386	166 257	158 781	169 709	137 139
Read depth	88 985	87 825	76 775	75 296	80 190	65 095

of the read depth and base count is displayed using GATK (www.broadinstitute.org/gatk/).

A total of 1 005 608 validated reads corresponding to six serial samples were analyzed by deep sequencing. The mean number of reads mapping on the HBV reference was 167 601 and the mean depth of each case was 79 028 (Table 2). The nine most variable amino acid substitutions, rt169, rt173, rt180, rt181, rt184, rt202, rt204, rt236 and rt250, known to be associated with NA resistance, were examined. The problem was how to differentiate true mutations from sequencing error in the obtained reads. Nishijima *et al.* tried to determine the PCR amplicon of the HBV genome derived from the expression plasmid to take the PCR-induced errors as well as sequencing errors into consideration. They described that the mean error rate was 0.034%, with the distribution of the per-nucleotide error rate ranging 0–0.13%.[26] Therefore, mutations over 1.0% were considered to be valid. First, rt180 of HBV-P10140 showed mixed variants in 76.9% of methionine with LAM-resistant mutations and in 23.1% of wild type with leucine, and rt204 also showed mixed variants in 69.0% of valine and 29.8% of isoleucine with LAM-resistant mutations, and in only 1.2% of wild-type methionine. During the NA treatment, the ratio of resistance mutations was increased, and rt180 of HBV-P12009 showed mixed variants in 96.8% of methionine with LAM-resistant mutations and rt204 also showed mixed variants in 96.2% of valine with LAM-resistant mutations. At rt184, related to ETV resistance, the resistant variants were detectable in 58.7% of the sequence, with replacement of leucine by wild-type threonine in HBV-P10140. Gradually, ETV-resistant variants increased and were detected in 82.3% of leucine in HBV-P12009. In addition, at rt202, the ration of serine with ETV mutants was increased from 1.3% to 3.4% during the treatment with NA (Fig. 1b). Of note, at rt169, rt173, rt181, rt236 and rt250, there were no NA-resistant mutations.

Then, we investigated the existence of drug-resistant HBV clones that could latently develop in patients. We enrolled seven patients treated with continuous NA for up to 2 years but in whom there was continual detection of viral copies in serum in this trial. Direct Sanger sequencing detected LAM-resistant mutations in five of the seven subjects. They had the following mutations: (i) rtL180M + rtM204V and (ii) rt180M and no mutations were found at rtV173L. However, by deep sequencing, in four subjects there was part of a mixture with rtL180L/M (35.4%/64.6%) and rtM204M/V (35.2%/64.8%) in HBV-P10036, with rtL180L/M (10.6%/86.8%) and rtM204M/V/I (0.0%/75.5%/24.5%) in HBV-P12043, with rtL180L/M (19.5%/80.5%) and rtM204M/V/I (4.4%/79.5%/16.1%) in HBV-P13064 and with rtL180L/M (23.4%/76.6%), rtM204M/V/I (23.2%/41.6%/35.2%) and one secondary minority variant of rtV173V/L (55.4%/44.6%) in HBV-P13061. Next, an ADV-resistant mutation of rtA181V was detected in two subjects by Sanger sequencing, and was present in 100.0% in HBV-P07061 and in 35.3% in HBV-P08463 by deep sequencing. In addition, minority variant ADV-resistant mutations were detected with 8.5% of rtA181V and with 14.5% of rtN236T in HBV-P10036, and with 2.1% of rtA181V in HBV-P13064. Of note, an ETV-resistant mutation appeared only in one subject with rtT184L by Sanger sequencing, while some low frequency ETV-resistant mutations were detected in four subjects by deep sequencing (Table 3). Therefore, the continual viremia of HBV treated with NA for long term may lead to NA-resistant mutations.

In conclusion, we demonstrated the amino acid substitutions of serial NA-resistant HBV by Sanger sequencing and MiSeq deep sequencing. We revealed that NA-resistant mutants appear unchanged at a glance but suggest the existence of low-abundant mutant clones that may develop drug resistance against NA through the selection of dominant mutations. The viral loads have decreased, but the effect of ETV is expected to be reduced. Further analysis by deep sequencing technologies is necessary to understand the significance and clinical relevance of viral mutations in the pathophysiology of NA-resistant HBV infection.

Table 3 HBV NA-resistant mutations detected by Sanger sequencing and deep sequencing

Sample	Treatment	HBV DNA (log copies/mL)	NA-resistant mutations	
			Sanger sequence	Deep sequence
HBV-P07061	LAM + ADV	5.0	A181V	**A181V (100.0%)**
HBV-P10036	ETV	2.5	L180M, M204V	V173M (1.3%), **L180M (64.6%)**, **A181V (8.5%)**, **T184S (4.5%)**, **S202C (2.3%)**, **M204V (64.8%)**, **N236T (14.3%)**
HBV-P08463	ETV	3.4	A181V	**A181V (35.3%)**
HBV-P12043	ETV	4.7	L180M, M204V	V173M (4.4%), **V173L (2.7%)**, **L180M (86.8%)**, L180Q (2.6%), **T184L (27.9%)**, **T184M (5.1%)**, **S202G (16.6%)**, **M204V (75.5%)**, **M204I (24.5%)**
HBV-P12081	LAM + ADV	2.9	L180M, T184L, M204V	I169A (25.4%), **L180M (100.0%)**, **T184L (100.0%)**, **M204V (100.0%)**
HBV-P13064	ETV	7.1	L180M, M204V	V173M (12.9%), **L180M (80.5%)**, **A181V (2.1%)**, **A181T (3.6%)**, **M204V (79.5%)**, **M204I (16.1%)**, **M250L (2.8%)**
HBV-P13061	ETV	2.3	L180M	**V173L (44.6%)**, **L180M (76.6%)**, **M204V (41.6%)**, **M204I (35.2%)**, **M250L (1.3%)**

Mutations in bold type at deep sequence section showed NA-resistant mutations that have already been reported.
ADV, adefovir dipivoxil; ETV, entecavir; HBV, hepatitis B virus; LAM, lamivudine; NA, nucleoside/nucleotide analog.

REFERENCES

1 EASL clinical practice guidelines: management of chronic hepatitis B virus infection. *J Hepatol* 2012; **57:** 167–85.
2 Pan CQ, Hu KQ, Tsai N. Long-term therapy with nucleoside/nucleotide analogues for chronic hepatitis B in Asian patients. *Antivir Ther* 2012; doi: 10.3851/IMP2481. [Epub ahead of print].
3 Yokosuka O, Kurosaki M, Imazeki F *et al.* Management of hepatitis B: consensus of the Japan Society of Hepatology 2009. *Hepatol Res* 2011; **41:** 1–21.
4 Lok ASF, McMahon BJ. Chronic hepatitis B: update 2009. *Hepatology* 2009; **50:** 661–2.
5 Zuckerman AJ. Hepatitis viruses. In: Baron S, ed. *Medical Microbiology*, 4th edn. Galveston (TX): University of Texas Medical Branch at Galveston, 1996; Chapter 70.
6 Kann M, Bischof A, Gerlich WH. In vitro model for the nuclear transport of the hepadnavirus genome. *J Virol* 1997; **71:** 1310–16.
7 Locarnini S. Molecular virology of hepatitis B virus. *Semin Liver Dis* 2004; **24** (Suppl 1): 3–10.
8 Werle-Lapostolle B, Bowden S, Locarnini S *et al.* Persistence of cccDNA during the natural history of chronic hepatitis B and decline during adefovir dipivoxil therapy. *Gastroenterology* 2004; **126:** 1750–8.
9 Wong DK, Yuen MF, Ngai VW, Fung J, Lai CL. One-year entecavir or lamivudine therapy results in reduction of hepatitis B virus intrahepatic covalently closed circular DNA levels. *Antivir Ther* 2006; **11:** 909–16.
10 Severini A, Liu XY, Wilson JS, Tyrrell DL. Mechanism of inhibition of duck hepatitis B virus polymerase by (-)-beta-L-2′,3′-dideoxy-3′-thiacytidine. *Antimicrob Agents Chemother* 1995; **39:** 1430–5.
11 Seigneres B, Aguesse-Germon S, Pichoud C *et al.* Duck hepatitis B virus polymerase gene mutants associated with resistance to lamivudine have a decreased replication capacity in vitro and in vivo. *J Hepatol* 2001; **34:** 114–22.
12 Seifer M, Hamatake RK, Colonno RJ, Standring DN. In vitro inhibition of hepadnavirus polymerases by the triphosphates of BMS-200475 and lobucavir. *Antimicrob Agents Chemother* 1998; **42:** 3200–8.
13 Inada M, Yokosuka O. Current antiviral therapies for chronic hepatitis B. *Hepatol Res* 2008; **38:** 535–42.
14 Allen MI, Deslauriers M, Andrews CW *et al.* Identification and characterization of mutations in hepatitis B virus resistant to lamivudine. Lamivudine Clinical Investigation Group. *Hepatology* 1998; **27:** 1670–7.
15 Fu L, Cheng YC. Role of additional mutations outside the YMDD motif of hepatitis B virus polymerase in L(-)SddC (3TC) resistance. *Biochem Pharmacol* 1998; **55:** 1567–72.
16 Fu L, Liu SH, Cheng YC. Sensitivity of L-(-)2,3-dideoxythiacytidine resistant hepatitis B virus to other antiviral nucleoside analogues. *Biochem Pharmacol* 1999; **57:** 1351–9.
17 Tenney DJ, Levine SM, Rose RE *et al.* Clinical emergence of entecavir-resistant hepatitis B virus requires additional substitutions in virus already resistant to Lamivudine. *Antimicrob Agents Chemother* 2004; **48:** 3498–507.
18 Tenney DJ, Rose RE, Baldick CJ *et al.* Long-term monitoring shows hepatitis B virus resistance to entecavir in

nucleoside-naive patients is rare through 5 years of therapy. *Hepatology* 2009; **49:** 1503–14.
19 Locarnini S. Primary resistance, multidrug resistance, and cross-resistance pathways in HBV as a consequence of treatment failure. *Hepatol Int* 2008; **2:** 147–51.
20 Bartholomeusz A, Tehan BG, Chalmers DK. Comparisons of the HBV and HIV polymerase, and antiviral resistance mutations. *Antivir Ther* 2004; **9:** 149–60.
21 Yatsuji H, Suzuki F, Sezaki H *et al.* Low risk of adefovir resistance in lamivudine-resistant chronic hepatitis B patients treated with adefovir plus lamivudine combination therapy: two-year follow-up. *J Hepatol* 2008; **48:** 923–31.
22 Ninomiya M, Ueno Y, Funayama R *et al.* Use of illumina deep sequencing technology to differentiate hepatitis C virus variants. *J Clin Microbiol* 2012; **50:** 857–66.
23 Danel C, Moh R, Chaix ML *et al.* Two-months-off, four-months-on antiretroviral regimen increases the risk of resistance, compared with continuous therapy: a randomized trial involving West African adults. *J Infect Dis* 2009; **199:** 66–76.
24 Takahashi M, Nishizawa T, Gotanda Y *et al.* High prevalence of antibodies to hepatitis A and E viruses and viremia of hepatitis B, C, and D viruses among apparently healthy populations in Mongolia. *Clin Diagn Lab Immunol* 2004; **11:** 392–8.
25 Langmead B, Salzberg SL. Fast gapped-read alignment with Bowtie 2. *Nat Methods* 2012; **9:** 357–9.
26 Nishijima N, Marusawa H, Ueda Y *et al.* Dynamics of hepatitis B virus quasispecies in association with nucleos(t)ide analogue treatment determined by ultra-deep sequencing. *PLoS ONE* 2012; **7:** e35052.

Novel Insights from Clinical Practice

HORMONE RESEARCH IN PÆDIATRICS

Horm Res Paediatr 2014;81:139–144
DOI: 10.1159/000355380

Received: July 12, 2013
Accepted: August 30, 2013
Published online: November 20, 2013

De novo Frameshift Mutation in *Fibroblast Growth Factor 8* in a Male Patient with Gonadotropin Deficiency

Erina Suzuki[a] Shuichi Yatsuga[d] Maki Igarashi[a] Mami Miyado[a] Kazuhiko Nakabayashi[b] Keiko Hayashi[b] Kenichirou Hata[b] Akihiro Umezawa[c] Gen Yamada[e] Tsutomu Ogata[a, f] Maki Fukami[a]

Departments of [a]Molecular Endocrinology and [b]Maternal-Fetal Biology, National Research Institute for Child Health and Development, [c]Department of Reproductive Biology, Center for Regenerative Medicine, National Research Institute for Child Health and Development, Tokyo, [d]Department of Pediatrics and Child Health, Kurume University School of Medicine, Kurume, [e]Department of Developmental Genetics, Institute of Advanced Medicine, Wakayama Medical University, Wakayama, and [f]Department of Pediatrics, Hamamatsu University School of Medicine, Hamamatsu, Japan

Established Facts

- Missense, nonsense, and splice mutations in *Fibroblast Growth Factor 8 (FGF8)* have been identified in patients with hypothalamo-pituitary dysfunction and craniofacial anomalies.

Novel Insights

- *FGF8* frameshift mutations account for a part of the etiology of hypothalamo-pituitary dysfunction and craniofacial anomalies.
- Micropenis in patients with *FGF8* mutations can be ascribed to gonadotropin deficiency and impaired outgrowth of the anlage of the penis.

Key Words
Fibroblast Growth Factor 8 · Frameshift mutation · Gonadotropin deficiency · Hypothalamo-pituitary dysfunction

Abstract
Background/Aims: Missense, nonsense, and splice mutations in the *Fibroblast Growth Factor 8 (FGF8)* have recently been identified in patients with hypothalamo-pituitary dysfunction and craniofacial anomalies. Here, we report a male patient with a frameshift mutation in *FGF8*. ***Case Report:*** The patient exhibited micropenis, craniofacial anomalies, and ventricular septal defect at birth. Clinical evaluation at 16 years and 8 months of age revealed delayed puberty, hyposmia, borderline mental retardation, and mild hearing difficulty. Endocrine findings included gonadotropin deficiency and primary hypothyroidism. ***Results:*** Molecular analysis identified a de novo heterozygous p.S192fsX204 mutation in the last exon of *FGF8*. RT-PCR analysis of normal human tissues detected *FGF8* expression in the genital skin, and whole-mount in situ hybridization analysis of mouse embryos revealed *Fgf8* expression in the anlage of the penis. ***Conclusion:*** The results indicate that frameshift mutations in *FGF8* account for a part of the etiology of hypothalamo-pituitary dysfunction. Micropenis in patients with *FGF8* abnormalities appears to be caused by gonadotropin deficiency and defective outgrowth of the anlage of the penis.

E. Suzuki, S. Yatsuga and M. Igarashi contributed equally to this work.

KARGER

© 2013 S. Karger AG, Basel
1663–2818/13/0812–0139$38.00/0

E-Mail karger@karger.com
www.karger.com/hrp

Maki Fukami, MD
Department of Molecular Endocrinology
National Research Institute for Child Health and Development
2-10-1 Ohkura, Setagaya, Tokyo 157-8535 (Japan)
E-Mail fukami-m@ncchd.go.jp

Introduction

Fibroblast growth factor (FGF) 8 (FGF8, NP_149353.1) is the major ligand of FGF receptor 1 (FGFR1) and plays a critical role in formation of the anterior midline in the forebrain [1–5]. Animal studies have indicated that FGF8 regulates the development of GnRH neurons in a dose-dependent manner [4, 5]. Recently, multiple missense mutations as well as two nonsense and one splice mutation in *FGF8* (NM_033163.3) have been identified in patients with various types of hypothalamo-pituitary dysfunction and craniofacial anomalies [1, 3, 4–9]. The mutation-positive patients invariably manifest gonadotropin deficiency and/or delayed puberty, indicating that GnRH neurons are highly vulnerable to impaired function of FGF8 [1, 3, 4–9]. Furthermore, mutations in several genes involved in the FGF8–FGFR1 network have been shown to underlie gonadotropin deficiency [1].

However, given the small number of reported patients, further studies are necessary to clarify the mutation spectrum and phenotypes of *FGF8* abnormalities. For example, frameshift mutations in *FGF8* have not been identified, and the underlying mechanisms of genital anomalies in patients with *FGF8* mutations have poorly been investigated. Here, we report a male patient with a de novo frameshift mutation in *FGF8*.

Subjects and Methods

Case Report

The male patient was born to non-consanguineous Japanese parents at 38 weeks' gestation. At birth, the patient manifested micropenis, phimosis, and hypoplastic scrotum. He also exhibited cleft lip and palate, strabismus, and ventricular septal defect. Hypospadias and cryptorchidism were absent. From 6 months of age, he underwent surgical interventions for facial and genital abnormalities. He had multiple episodes of convulsions from 12 years of age, and was treated with anticonvulsants. From infancy to early teens, his stature followed the –2.0 SD growth curve for Japanese males (fig. 1a).

At 16 years and 8 months of age, the patient was referred to our clinic for delayed puberty. Clinical assessment revealed a high-pitched voice and pubic and axillary hair of Tanner stage 1–2. His penile length was 1.5 cm (fig. 1b). Bilateral testes of ~1 ml were palpable in the scrotum. His stature and weight were 154.0 cm (–2.8 SD) and 52.9 kg (–0.8 SD), respectively. He had mild hearing difficulty and borderline mental retardation with a WISC-III IQ score of 71. Although he showed a response to a smell test using intravenous injection of combined vitamins (Alinamin; Takeda Pharmaceutical Co. Ltd, Osaka, Japan), he was unable to identify various odorants. Thus, he was suspected as having hyposmia. Brain magnetic resonance imaging delineated no structural abnormalities in the hypothalamus, pituitary, or olfactory bulbs (fig. 1b). The patient manifested no symptoms associated with the heart anomaly, although cardiac evaluation showed a ventricular septal defect of approximately 2 mm. His father, mother and elder brother were clinically normal, and had heights of 164 cm (–1.2 SD), 143 cm (–2.7 SD), and 167 cm (–0.7 SD), respectively.

Endocrine examinations indicated multiple hormone deficiencies in the patient (table 1). Blood LH values were low at baseline and poorly responded to GnRH stimulation. FSH values were low-normal. Slightly elevated TSH levels and mildly decreased free T_4 levels indicated primary hypothyroidism. The IGF-1 level was low-normal. Blood levels of prolactin, ACTH, and cortisol were within the normal range. Anti-thyroperoxidase and anti-thyroglobulin antibodies were negative. Thyroid technetium-99m scintigram revealed no abnormalities. After initiation of levothyroxine supplementation therapy (50 μg/day), TSH and free T_4 values remained within the normal range.

Mutation Analysis

This study was approved by the Institutional Review Board Committee at the National Center for Child Health and Development and performed after obtaining written informed consent. A genomic DNA sample from the patient was analyzed for mutations in 13 genes that have been implicated in gonadotropin deficiency: *FGFR1*, *KAL1*, *FGF8*, *PROK2*, *PROKR2*, *TAC3*, *TACR3*, *KISS1*, *KISS1R*, *GNRHR*, *GNRH1*, *CHD7*, and *NELF* [1, 7, 10, 11]. Mutations were screened by the Haloplex method (Agilent Technologies, Palo Alto, Calif., USA) on a MiSeq next-generation sequencer (Illumina, San Diego, Calif., USA). An *FGF8* mutation indicated by the screening analysis was confirmed by Sanger sequencing with primers, 5′-GCGAGTTGTGAGGGATTAGAGA-3′ and 5′-GGGTGCCCTACAGGATGAG-3′. To verify the heterozygous mutation, the PCR product was subcloned into a TOPO TA cloning vector (Life Technologies, Carlsbad, Calif., USA) and the mutant and wild-type alleles were sequenced separately. Genomic DNA samples from the parents and brother were examined for the presence or absence of the *FGF8* mutation.

Expression Analysis for FGF8/Fgf8 in Normal Human Tissues and Mouse Embryos

We investigated mRNA expression of *FGF8* in normal human tissues by PCR. Human cDNA samples were purchased from Clontech (Palo Alto, Calif., USA) or prepared by RT-PCR. PCR analysis of *FGF8* was performed with primers, 5′-AGTCCGAGGAGCCGAGA-3′ and 5′-AAGTGGACCTCACGCTGGT-3′. As an internal control, we amplified *GAPDH* with primers, 5′-CCACCCATGGCAAATTCCATGGCA-3′ and 5′-TCTAGACGGCAGGTCAGGTCCACC-3′.

We also examined the expression of *Fgf8* in the developing external genitalia of mouse embryos by whole-mount in situ hybridization. An antisense cRNA fragment corresponding to nucleotide 1–978 of mouse *Fgf8* (BC048734) was utilized as a probe. The procedures were performed as described previously [12].

Results

Mutation Analysis

The patient carried a heterozygous frameshift mutation in the last exon of *FGF8* (p.S192fsX204, c.574delT)

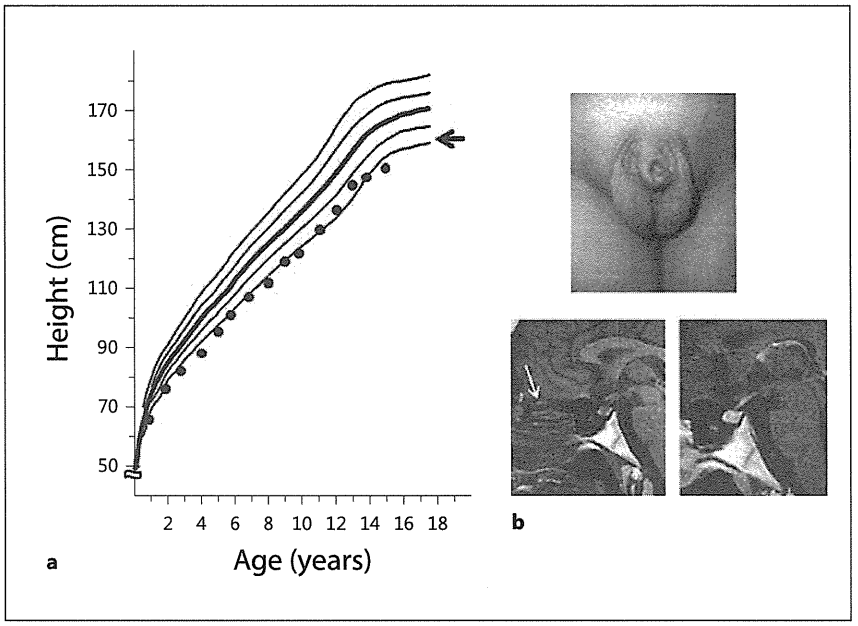

Fig. 1. Clinical findings of the patient. **a** Growth chart. Actual height of the patient is plotted against the growth curve for Japanese boys (the mean, ±1.0 SD and ±2.0 SD). The arrow indicates the midparental height. **b** Upper panel: genital appearance at 16 years and 8 months of age. Lower panels: brain magnetic resonance imaging. No abnormalities are detected in the hypothalamus, pituitary, or olfactory bulbs (arrow).

Table 1. Endocrine data of the patient

	Stimulus (dosage)	Patient		Reference values[1]	
		baseline	peak	baseline	peak
At diagnosis					
LH, mIU/ml	GnRH (100 μg)[2]	**0.5**	**4.6**	0.8–4.2	18.2–38.0
FSH, mIU/ml	GnRH (100 μg)[2]	3.0	9.5	2.9–10.8	5.8–22.3
GH, ng/ml	Insulin (3 U)[2]	0.87	**3.18**[3]	0.6–8.7	>6.0
Prolactin, ng/ml	TRH (350 μg)[2]	4.3	14.4	1.1–9.5	–
TSH, μU/ml	TRH (350 μg)[2]	*8.3*	23.0	0.6–5.9	5.8–30.6
IGF-1, ng/ml		301[4]	–	250–680	–
ACTH, pg/ml	CRH (100 μg)[2]	9.5	50.3	5.3–51.1	17.2–153.3
Cortisol, μg/dl	CRH (100 μg)[2]	8.4	25.8	3.9–21.3	13.1–35.6
Free T_4, ng/dl		**0.79**	–	1.0–1.7	–
Free T_3, pg/ml		2.8	–	2.1–4.1	–
Testosterone, ng/ml	HCG (4,000 U)[5]	**0.12**	**0.38**	2.8–7.0	11.0–13.1
On levothyroxine treatment[6]					
TSH, μU/ml		0.68	–	0.6–5.9	–
Free T_4, ng/dl		1.14	–	1.0–1.7	–

The conversion factors to the SI unit: LH, 1.0 (IU/l); FSH, 1.0 (IU/l); GH, 1.0 (μg/l); prolactin, 43.48 (pmol/l); TSH, 1.0 (mIU/l); IGF-I, 0.131 (nmol/l); ACTH, 0.22 (pmol/l); cortisol, 27.59 (nmol/l); free T_4, 12.87 (pmol/l); free T_3, 1.54 (pmol/l), and testosterone, 3.47 (nmol/l). Hormone values above the reference range are italicized and those below the reference range are boldfaced.

[1] Reference values in age-matched males. [2] GnRH, insulin and TRH i.v.; blood sampling at 0, 30, 60, 90, and 120 min. [3] Low GH values of the patient may be due to insufficient hypoglycemic stimulation; blood glucose was 89 mg/dl at 0 min, and 58 mg/dl at 30 min. [4] –1.7 SD. [5] HCG i.m. for 3 consecutive days; blood sampling on days 1 and 4. [6] Levothyroxine 50 μg/day.

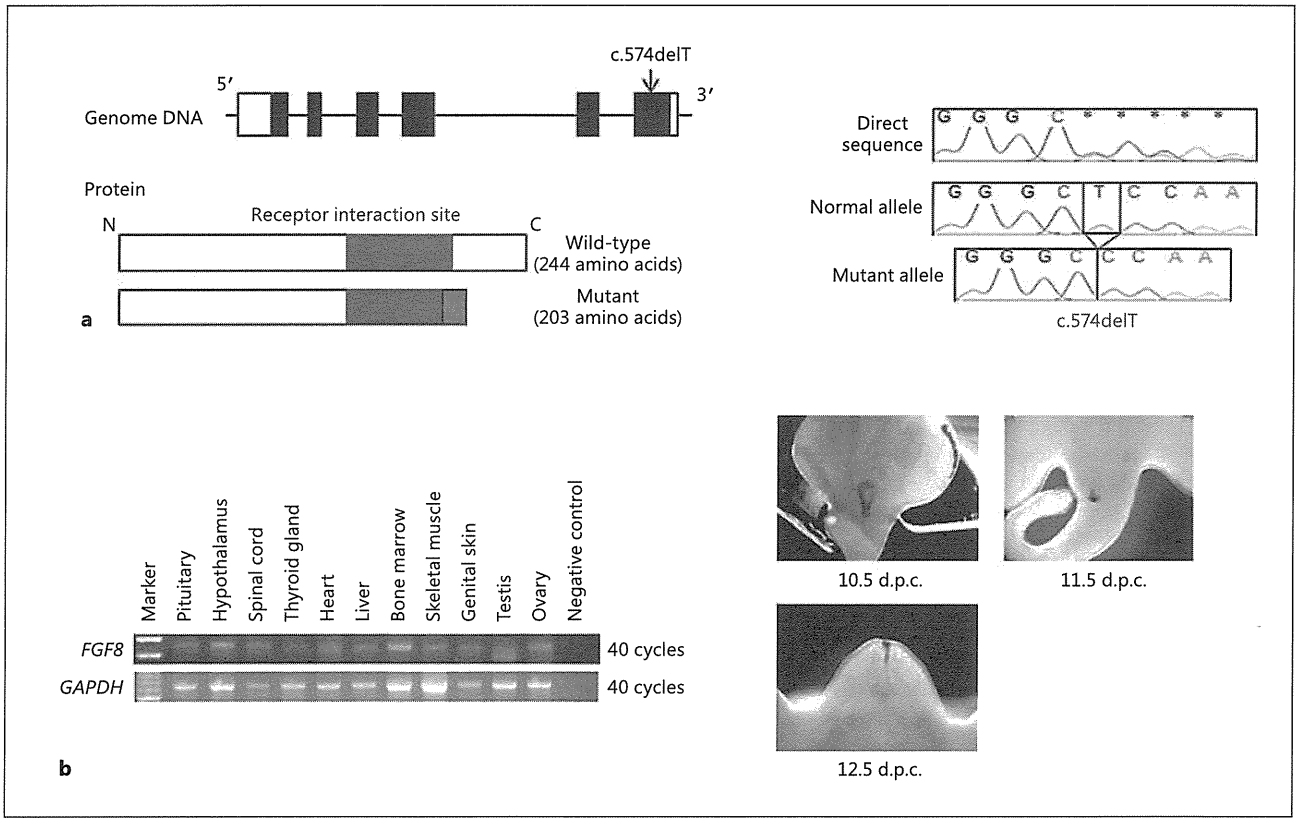

Fig. 2. Mutation analysis of *FGF8* and expression studies of *FGF8/Fgf8*. **a** *FGF8* mutation identified in the patient. The positions of nucleotides and amino acids correspond to NM_033163.3 and NP_149353.1, respectively. Left panel: the genomic and protein structures of FGF8. The white and black boxes in genome DNA indicate the non-coding and coding regions, respectively. The blue boxes in the protein depict the receptor interaction site at codons 83–207 and the red box indicates truncated amino acids. Right panel: chromatograms of the c.574delT mutation. **b** Expression analyses of *FGF8/Fgf8*. Left panel: PCR-based cDNA screening for human *FGF8*. After 40 cycles, PCR products for *FGF8* were detected in all tissues examined. *GAPDH* is utilized as an internal control. Right panel: whole-mount in situ hybridization analysis in mouse embryos. Purple signals indicate expression of mouse *Fgf8*. d.p.c. = Days post-coitum.

(fig. 2a). No pathogenic mutations were identified in other tested genes. The p.S192fsX204 mutation was predicted to truncate the C-terminus of FGF8 by replacing 53 amino acids with 12 aberrant amino acids (fig. 2a). This mutation affected a part of the receptor interacting site of FGF8 (codons 83–207). The *FGF8* mutation was not identified in the parents or brother.

Expression Analysis for FGF8/Fgf8 in Normal Human Tissues and Mouse Embryos

PCR-based cDNA screening indicated that human *FGF8* is expressed in a range of tissues including the hypothalamus, pituitary, thyroid gland, heart, and genital skin (fig. 2b). Whole-mount in situ hybridization indicated that mouse *Fgf8* is expressed in the epithelium of the outmost part of the urogenital sinus before outgrowth of the anlage of the penis (genital tubercle) (10.5 days post-coitum) and in the epithelium of distal urethral plate during development of the genital tubercle (11.5 and 12.5 days post-coitum) (fig. 2b).

Discussion

We identified a de novo *FGF8* frameshift mutation in a Japanese patient with gonadotropin deficiency and multiple complications. The p.S192fsX204 mutation resides in the last exon of *FGF8* and is likely to escape non-

sense-mediated mRNA decay [13]. However, the mutation is predicted to alter the C-terminal structure of the protein and affect the receptor interacting site. In this context, Falardeau et al. [4] indicated that a missense mutation at the 229th codon is sufficient to reduce in vitro activity. Thus, although in vitro functional assays have not been conducted for p.S192fsX204, this mutation appears to markedly impair the function of FGF8. Consistent with this, the patient manifested gonadotropin deficiency, hyposmia, and craniofacial anomalies comparable to the phenotypes of previously reported patients with nonsense, missense, and splice mutations of *FGF8* [1, 3–9]. These data indicate for the first time that frameshift mutations of *FGF8* account for a part of the etiology of hypothalamo-pituitary dysfunction and craniofacial anomalies.

We cannot exclude the possibility that the patient carries additional mutations in other genes involved in hypothalamo-pituitary function. Although *FGF8* abnormalities are known to cause gonadotropin deficiency mostly as monoallelic mutations, they can also appear in an oligogenic condition [1]. Therefore, although our patient has no mutations in the 13 known causative genes for gonadotropin deficiency, he may have mutations in other unexamined genes. Indeed, several genes including *FGF17*, *IL17RD*, *DUSP6*, *SPRY4*, and *FLRT3* have recently been implicated in gonadotropin deficiency [1].

The Japanese patient manifested severe micropenis. This phenotype is consistent with severe gonadotropin deficiency [14]. In addition, defective formation the penis during fetal period may have played a role in the development of micropenis, because outgrowth of the genital tubercle in mouse embryos primarily depends on *Fgf8* signaling [12]. Indeed, we found expression of *FGF8/Fgf8* in human genital skin and in the epithelium of the mouse genital tubercle.

The patient manifested primary hypothyroidism and a congenital heart anomaly, neither of which has been reported in patients with *FGF8* mutations. Although we detected expression of *FGF8* in the human thyroid gland and heart, and several studies have revealed that FGF8 plays an essential role in formation of the cardiovascular system and thyroid gland in mice [15–20], it remains unknown whether thyroid and heart abnormalities of the patient are associated with the *FGF8* mutation.

In summary, we identified the first frameshift *FGF8* mutations in a patient with gonadotropin deficiency. The results indicate molecular diversity of *FGF8* abnormalities.

Acknowledgements

This work was supported by grants from the Ministry of Health, Labor and Welfare and from Takeda Science Foundation, by Grant-in-Aid for Scientific Research from the Japan Society for the Promotion of Science, by Grant-in-Aid for Scientific Research on Innovative Areas from the Ministry of Education, Culture, Sports, Science and Technology and by the Grant of National Center for Child Health and Development.

Disclosure Statement

The authors have no conflicts of interest to disclose.

References

1 Miraoui H, Dwyer AA, Sykiotis GP, Plummer L, Chung W, Feng B, Beenken A, Clarke J, Pers TH, Dworzynski P, Keefe K, Niedziela M, Raivio T, Crowley WF Jr, Seminara SB, Quinton R, Hughes VA, Kumanov P, Young J, Yialamas MA, Hall JE, Van Vliet G, Chanoine JP, Rubenstein J, Mohammadi M, Tsai PS, Sidis Y, Lage K, Pitteloud N: Mutations in FGF17, IL17RD, DUSP6, SPRY4, and FLRT3 are identified in individuals with congenital hypogonadotropic hypogonadism. Am J Hum Genet 2013;92:725–743.

2 Goetz R, Ohnishi M, Ding X, Kurosu H, Wang L, Akiyoshi J, Ma J, Gai W, Sidis Y, Pitteloud N, Kuro-O M, Razzaque MS, Mohammadi M: Klotho coreceptors inhibit signaling by paracrine fibroblast growth factor 8 subfamily ligands. Mol Cell Biol 2012;32:1944–1954.

3 Miraoui H, Dwyer A, Pitteloud N: Role of fibroblast growth factor signaling in the neuroendocrine control of human reproduction. Mol Cell Endocrinol 2011;346:37–43.

4 Falardeau J, Chung WC, Beenken A, Raivio T, Plummer L, Sidis Y, Jacobson-Dickman EE, Eliseenkova AV, Ma J, Dwyer A, Quinton R, Na S, Hall JE, Huot C, Alois N, Pearce SH, Cole LW, Hughes V, Mohammadi M, Tsai P, Pitteloud N: Decreased FGF8 signaling causes deficiency of gonadotropin-releasing hormone in humans and mice. J Clin Invest 2008;118:2822–2831.

5 McCabe MJ, Gaston-Massuet C, Tziaferi V, Gregory LC, Alatzoglou KS, Signore M, Pueles E, Gerrelli D, Farooqi IS, Raza J, Walker J, Kavanaugh SI, Tsai PS, Pitteloud N, Martinez-Barbera JP, Dattani MT: Novel FGF8 mutations associated with recessive holoprosencephaly, craniofacial defects, and hypothalamo-pituitary dysfunction. J Clin Endocrinol Metab 2011;96:E1709–E1718.

6 Raivio T, Avbelj M, McCabe MJ, Romero CJ, Dwyer AA, Tommiska J, Sykiotis GP, Gregory LC, Diaczok D, Tziaferi V, Elting MW, Padidela R, Plummer L, Martin C, Feng B, Zhang C, Zhou QY, Chen H, Mohammadi M, Quinton R, Sidis Y, Radovick S, Dattani MT, Pitteloud N: Genetic overlap in Kallmann syndrome, combined pituitary hormone deficiency, and septo-optic dysplasia. J Clin Endocrinol Metab 2012;97:E694–E699.

7 Sykiotis GP, Plummer L, Hughes VA, Au M, Durrani S, Nayak-Young S, Dwyer AA, Quinton R, Hall JE, Gusella JF, Seminara SB, Crowley WF Jr, Pitteloud N: Oligogenic basis of isolated gonadotropin-releasing hormone deficiency. Proc Natl Acad Sci USA 2010;107:15140–15144.

8 Trarbach EB, Abreu AP, Silveira LF, Garmes HM, Baptista MT, Teles MG, Costa EM, Mohammadi M, Pitteloud N, Mendonca BB, Latronico AC: Nonsense mutations in FGF8 gene causing different degrees of human gonadotropin-releasing deficiency. J Clin Endocrinol Metab 2010;95:3491–3496.

9 Arauz RF, Solomon BD, Pineda-Alvarez DE, Gropman AL, Parsons JA, Roessler E, Muenke M: A hypomorphic allele in the FGF8 gene contributes to holoprosencephaly and is allelic to gonadotropin-releasing hormone deficiency in humans. Mol Syndromol 2010;1:59–66.

10 Topaloglu AK, Kotan LD: Molecular causes of hypogonadotropic hypogonadism. Curr Opin Obstet Gynecol 2010;22:264–270.

11 Beate K, Joseph N, Nicolas de R, Wolfram K: Genetics of isolated hypogonadotropic hypogonadism: role of GnRH receptor and other genes. Int J Endocrinol 2012;2012:147893.

12 Haraguchi R, Suzuki K, Murakami R, Sakai M, Kamikawa M, Kengaku M, Sekine K, Kawano H, Kato S, Ueno N, Yamada G: Molecular analysis of external genitalia formation: the role of fibroblast growth factor (Fgf) genes during genital tubercle formation. Development 2000;127:2471–2479.

13 Kuzmiak HA, Maquat LE: Applying nonsense-mediated mRNA decay research to the clinic: progress and challenges. Trends Mol Med 2006;12:306–316.

14 Melmed S, Kleinberg D, Ho K: Pituitary physiology and diagnostic evaluation; in Melmed S, Polonsky KS, Larson PR, Kronenberg HM (eds): Williams Textbook of Endocrinology, ed 12. Philadelphia, Saunders, 2011, pp 175–228.

15 Park EJ, Watanabe Y, Smyth G, Miyagawa-Tomita S, Meyers E, Klingensmith J, Camenisch T, Buckingham M, Moon AM: An FGF autocrine loop initiated in second heart field mesoderm regulates morphogenesis at the arterial pole of the heart. Development 2008;135:3599–3610.

16 Wendl T, Adzic D, Schoenebeck JJ, Scholpp S, Brand M, Yelon D, Rohr KB: Early developmental specification of the thyroid gland depends on han-expressing surrounding tissue and on FGF signals. Development 2007;134:2871–2879.

17 Watanabe Y, Miyagawa-Tomita S, Vincent SD, Kelly RG, Moon AM, Buckingham ME: Role of mesodermal FGF8 and FGF10 overlaps in the development of the arterial pole of the heart and pharyngeal arch arteries. Circ Res 2010;106:495–503.

18 Lania G, Zhang Z, Huynh T, Caprio C, Moon AM, Vitelli F, Baldini A: Early thyroid development requires a Tbx1-Fgf8 pathway. Dev Biol 2009;328:109–117.

19 Abu-Issa R, Smyth G, Smoak I, Yamamura K, Meyers EN: Fgf8 is required for pharyngeal arch and cardiovascular development in the mouse. Development 2002;129:4613–4625.

20 Meyers EN, Lewandoski M, Martin GR: An Fgf8 mutant allelic series generated by Cre- and Flp-mediated recombination. Nat Genet 1998;18:136–141.

Mutations in *SERPINB7*, Encoding a Member of the Serine Protease Inhibitor Superfamily, Cause Nagashima-type Palmoplantar Keratosis

Akiharu Kubo,[1,2,3,*] Aiko Shiohama,[1,4] Takashi Sasaki,[1,2,3] Kazuhiko Nakabayashi,[5] Hiroshi Kawasaki,[1] Toru Atsugi,[1,6] Showbu Sato,[1] Atsushi Shimizu,[7] Shuji Mikami,[8] Hideaki Tanizaki,[9] Masaki Uchiyama,[10] Tatsuo Maeda,[10] Taisuke Ito,[11] Jun-ichi Sakabe,[11] Toshio Heike,[12] Torayuki Okuyama,[13] Rika Kosaki,[14] Kenjiro Kosaki,[15] Jun Kudoh,[16] Kenichiro Hata,[5] Akihiro Umezawa,[17] Yoshiki Tokura,[11] Akira Ishiko,[18] Hironori Niizeki,[19] Kenji Kabashima,[9] Yoshihiko Mitsuhashi,[10] and Masayuki Amagai[1,2,4]

"Nagashima-type" palmoplantar keratosis (NPPK) is an autosomal recessive nonsyndromic diffuse palmoplantar keratosis characterized by well-demarcated diffuse hyperkeratosis with redness, expanding on to the dorsal surfaces of the palms and feet and the Achilles tendon area. Hyperkeratosis in NPPK is mild and nonprogressive, differentiating NPPK clinically from Mal de Meleda. We performed whole-exome and/or Sanger sequencing analyses of 13 unrelated NPPK individuals and identified biallelic putative loss-of-function mutations in *SERPINB7*, which encodes a cytoplasmic member of the serine protease inhibitor superfamily. We identified a major causative mutation of c.796C>T (p.Arg266*) as a founder mutation in Japanese and Chinese populations. SERPINB7 was specifically present in the cytoplasm of the stratum granulosum and the stratum corneum (SC) of the epidermis. All of the identified mutants are predicted to cause premature termination upstream of the reactive site, which inhibits the proteases, suggesting a complete loss of the protease inhibitory activity of SERPINB7 in NPPK skin. On exposure of NPPK lesional skin to water, we observed a whitish spongy change in the SC, suggesting enhanced water permeation into the SC due to overactivation of proteases and a resultant loss of integrity of the SC structure. These findings provide an important framework for developing pathogenesis-based therapies for NPPK.

The congenital palmoplantar keratoses (PPKs) are a heterogeneous group of diseases. Phenotypic classification of hereditary PPKs is based mainly on the specific morphology and distribution of the hyperkeratosis, the presence or absence of associated features, and the inheritance pattern and is assisted by additional criteria such as the presence of skin lesions in areas other than the palms and soles, the age at onset of the hyperkeratosis, the severity of the disease process, and histopathological findings.[1]

"Keratosis palmoplantaris Nagashima"[2] or "Nagashima-type" PPK (NPPK)[3] has been proposed as a clinical entity included within the diffuse hereditary PPKs without associated features.[1] A familial case of two siblings was first reported as a distinct clinical type of PPK in 1989.[2,4] Because Nagashima briefly described this type of hereditary PPK in the Japanese literature in 1977,[5] the name "keratosis palmoplantaris Nagashima" was proposed.[2] Although about 20 cases of Japanese individuals with NPPK have been reported in the Japanese literature since then, this clinical entity was not described in detail in the English language literature until 2008.[3]

An autosomal recessive trait has been suggested in NPPK.[2,3] The clinical features of NPPK are characterized by well-demarcated reddish and diffuse palmoplantar hyperkeratosis that extends to the dorsal surfaces of the hands, feet, inner wrists, ankles, and the Achilles tendon area.[2–6] Involvement of the elbows and knees and high frequencies of hyperhidrosis on palms and soles have been noted.[3] Clinical observations revealed no differences between males and females, no seasonal change, and no association with squamous cell carcinoma or any other malignancy. Although mild T cell infiltration in the affected skin area has been reported,[7] the pathophysiology of the skin redness and hyperkeratosis are still uncharacterized.

An autosomal recessive trait, transgressive diffuse hyperkeratosis, and the absence of associated features are also characteristic of Mal de Meleda (MDM [MIM 248300]),[8] PPK Gamborg Nielsen (Norrbotten recessive type PPK [MIM 244850]),[9,10] and acral keratoderma.[11] These other

[1]Department of Dermatology, Keio University School of Medicine, Tokyo 160-8582, Japan; [2]Keio-Maruho Laboratory of Skin Barriology, Keio University School of Medicine, Tokyo 160-8582, Japan; [3]Center for Integrated Medical Research, Keio University School of Medicine, Tokyo 160-8582, Japan; [4]MSD Endowed Program for Allergy Research, Keio University School of Medicine, Tokyo 160-8582, Japan; [5]Department of Maternal-Fetal Biology, National Research Institute for Child Health and Development, Tokyo 157-8535, Japan; [6]KOSÉ Corporation, Tokyo 174-0051, Japan; [7]Department of Molecular Biology, Keio University School of Medicine, Tokyo 160-8582, Japan; [8]Division of Diagnostic Pathology, Keio University Hospital, Tokyo 160-8582, Japan; [9]Department of Dermatology, Kyoto University Graduate School of Medicine, Kyoto 606-8507, Japan; [10]Department of Dermatology, Tokyo Medical University, Tokyo 160-0023, Japan; [11]Department of Dermatology, Hamamatsu University School of Medicine, Hamamatsu 431-3192, Japan; [12]Department of Pediatrics, Kyoto University Graduate School of Medicine, Kyoto 606-8507, Japan; [13]Department of Laboratory Medicine, National Center for Child Health and Development, Tokyo 157-8535, Japan; [14]Department of Clinical Genetics, National Center for Child Health and Development, Tokyo 157-8535, Japan; [15]Center for Medical Genetics, Keio University School of Medicine, Tokyo 160-8582, Japan; [16]Laboratory of Gene Medicine, Keio University School of Medicine, Tokyo 160-8582, Japan; [17]Department of Reproductive Biology, National Research Institute for Child Health and Development, Tokyo 157-8535, Japan; [18]Department of Dermatology, School of Medicine, Toho University, Tokyo 143-8540, Japan; [19]Department of Dermatology, National Center for Child Health and Development, Tokyo 157-8535, Japan
*Correspondence: akiharu@a5.keio.jp
http://dx.doi.org/10.1016/j.ajhg.2013.09.015.

diffuse PPKs show more severe and more progressive features than does NPPK, such as thick hyperkeratosis, leading to flexion contractures (MDM) and constricting bands surrounding the digits (MDM, PPK Gamborg Nielsen, and acral keratoderma), occasionally resulting in spontaneous amputation (MDM and acral keratoderma).[1] NPPK shows only mild and nonprogressive hyperkeratosis and does not show flexion contractures or constricting bands. Thus, NPPK is distinguishable clinically from these other PPKs. Mutations in the coding region of the *SLURP1* (MIM 606119) have been identified in MDM but not in NPPK, suggesting that MDM and NPPK are genetically distinct diseases.[3,12]

To identify gene mutations responsible for NPPK, we performed whole-exome sequencing in three unrelated Japanese NPPK individuals (KDex8 [II-1 of family 1 in Figure 1A], KDex14 [II-2 of family 2], and KDex20 [II-3 of family 3]) who showed the characteristic symptoms of NPPK; Figures 1B and 1C; see Figure S1 available online. Clinical features are summarized in Table 1. The major clinical differentiating points by which we diagnosed these individuals with NPPK among the diverse hereditary PPKs without associated features are summarized in Table 2. The study was conducted after obtaining written informed consent according to the guidelines of the Institutional Review Board of Keio University School of Medicine, National Center for Child Health and Development, Kyoto University, and Tokyo Medical University in accordance with the Helsinki guidelines.

Whole-exome sequencing and data analyses were performed as described previously.[13] Whole-exome sequencing produced approximately 100,000,000 paired reads per sample, approximately 80% of which were mapped to the hs37d5 exon region of the human genome sequence assembly.[14] The average coverage of the exonic region was 87.5×, with more than 93.2% of targeted bases covered at 10× reads. No *SLURP1* mutation (Refseq: NM_020427.2) was identified in any of the three NPPK individuals. A genome informatics study found 693, 677, and 747 allelic variants in three NPPK individuals (KDex8, 14, and 20, respectively), showing a minor allele frequency of less than 1% in the 1092 individuals from the 1000 Genomes Project.[14] Because NPPK is possibly inherited in an autosomal recessive manner,[2,3] the causative mutation was expected to be a homozygous or compound heterozygous variant shared by the affected individuals but absent or found only in a heterozygous manner in the control cohort. Among the identified variants, only mutations in the *SERPINB7* (MIM 603357) fulfilled these requirements, suggesting a causative role in NPPK (Table 1).

SERPINB7 consists of eight exons, with three distinct transcription start sites (exons 1a–c; Figure 2A). The start codon is located within exon 2, and the termination codon within exon 8 (Figure 2A). The *SERPINB7* transcript (RefSeq: NM_001040147.2) encodes a 380 amino-acid protein. Mutations identified by whole-exome sequencing were confirmed by Sanger sequencing by using the primers in Table S1 (Figure 2B). A nonsense mutation encoding a c.796C>T alteration (p.Arg266*) in the last exon of the *SERPINB7* was found in all three NPPK individuals. KDex20 was homozygous for the c.796C>T nonsense mutation. KDex8 was a compound heterozygote of a maternal c.796C>T mutation and a paternal small indel mutation of c.218_219delAGinsTAAACTTTACCT (c.218_219del2ins12) at the end of exon 3, predicted to lead to a premature stop codon (p.Gln73Leufs*17). KDex14 was a compound heterozygote of a maternal c.796C>T mutation and a paternal mutation of c.455-1G>A in the splice acceptor site upstream of exon 6 of *SERPINB7*, which was also predicted to lead to a premature stop codon (p.Gly152Valfs*21) at chromosome 18: 61465837 in the hs37d5 human genome sequence.[14]

To confirm mutations in *SERPINB7* as a cause of NPPK, we analyzed ten additional unrelated NPPK individuals. The clinical manifestations of these individuals are presented in Table 1. Sanger sequencing failed to detect a mutation in *SLURP1* in any of the ten individuals by using methods described previously.[3] When the entire coding region of *SERPINB7* was analyzed by Sanger sequencing with the primers in Table S1, five of the ten individuals were homozygous for the c.796C>T mutation, four were compound heterozygotes of the c.796C>T and c.218_219 del2ins12 mutations, and one was a compound heterozygote of the c.796C>T and c.455-1G>A mutations (Table 1). These results confirmed that mutations in *SERPINB7* are a major cause of NPPK and that c.796C>T and c.218_219 del2ins12 are major mutations for NPPK in a Japanese population.

From our clinical experience, NPPK is much more common than other types of hereditary PPKs in Japan, although no statistical analysis has been reported. NPPK has not been recognized as a clinical entity within PPKs in Western populations, probably because it is rare. Next, we evaluated the variant databases of the cohort of 1,092 individuals in the 1000 Genomes Project[14] to estimate the frequency of *SERPINB7* mutations classified by ethnicity. The nonsense mutation of c.796C>T was identified as an SNP (rs142859678) with a minor allele frequency of 0.4% and found in a heterozygous manner in two of 89 Japanese individuals, four of 97 Han Chinese individuals from Beijing, and two of 100 Han Chinese individuals from southern China. On the other hand, the c.796C>T mutation was not found in any of 806 non-Asian individuals, suggesting that the c.796C>T mutation is a founder mutation causing NPPK in Asian populations. We also found another putative causative mutation, c.336+2T>G (an SNP of rs201433665), in one of 97 Han Chinese individuals from Beijing in a heterozygous manner. Other mutations found in this study were not identified in the 1,092 individuals.

From these results, the prevalence rate of NPPK was estimated as 1.2/10,000 in Japanese populations and 3.1/10,000 in Chinese populations. In contrast, no putative causative mutation (nonsense, missense, insertion,

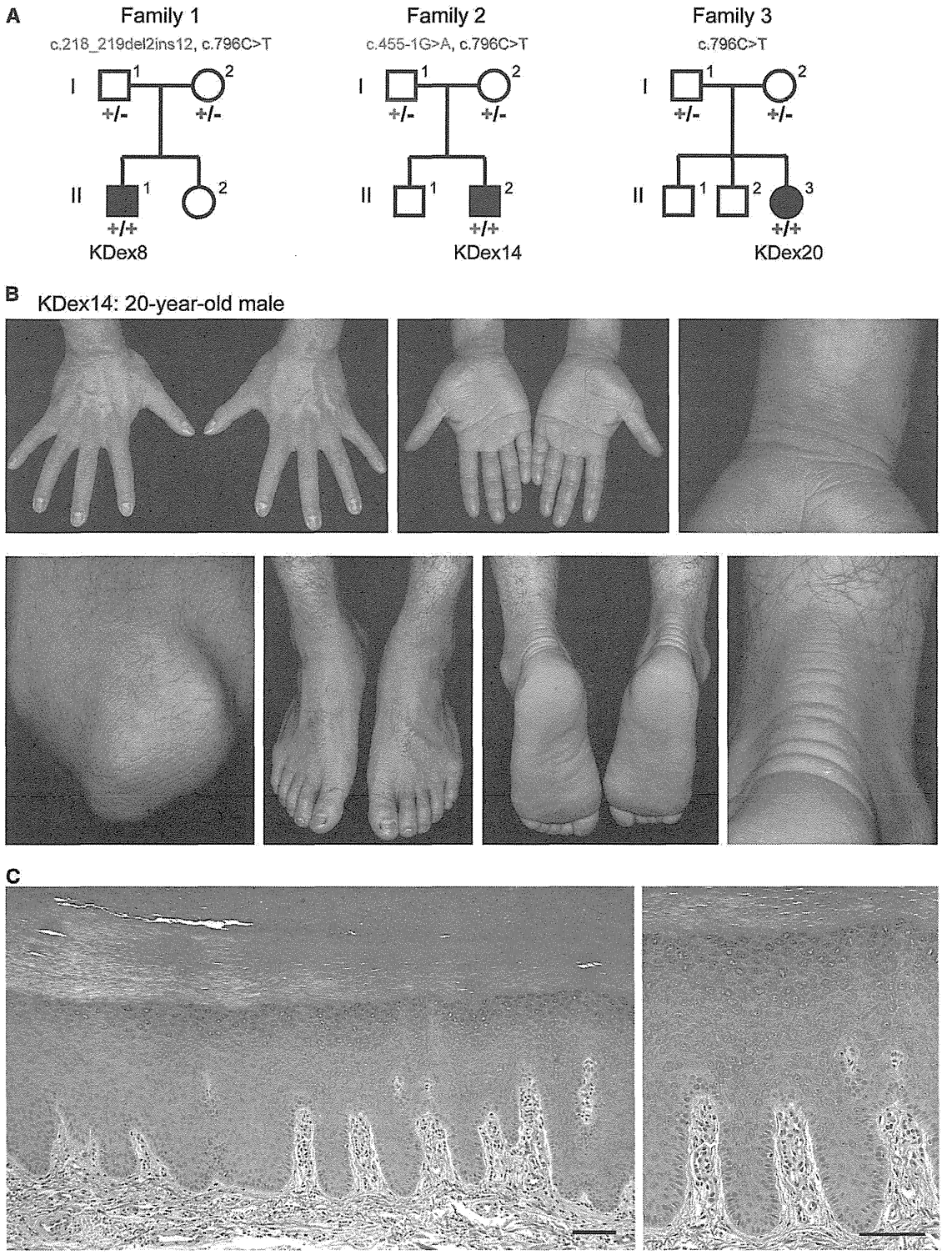

Figure 1. Family Pedigrees and Skin Manifestations of the Probands with NPPK
(A) Pedigrees for the families in which exome sequencing and analyses were performed on the probands (KDex8, KDex14, and KDex20). Segregation of the mutations identified in each pedigree is shown.
(B) Skin manifestations of the proband KDex14.
(C) Hematoxylin and eosin staining of the plantar epidermis of the proband KDex8. Scale bars represent 100 μm.

deletion, or exon-intron boundary mutation) was identified in 806 individuals of non-Asian origin in the 1000 Genomes Project.[14] We further searched causative mutations in European-American and African-American populations by using the NHBLI Exome Variant Server and found only one putative causative mutation, c.309delT in the exon 4 (1 of 12,517 alleles), predicted to lead to a premature stop codon (p.Phe103Leufs*33). Thus, the

Table 1. *SERPINB7* Mutations and Clinical Phenotypes in Individuals with NPPK

		Allele 1			Allele 2					
Affected Individual	**Gender / Age**	**Base Change**	**Amino Acid Change**	**Segregation**	**Base Change**	**Amino Acid Change**	**Segregation**	**Onset**	**Other Involved Areas**	**Hyperhidrosis**
Homozygous Mutations										
KDex20[a]	F/10	c.796C>T	p.Arg266*	Paternal	c.796C>T	p.Arg266*	Maternal	At birth	Knees	+
KDex55	F/2	c.796C>T	p.Arg266*	Paternal	c.796C>T	p.Arg266*	Maternal	Early infancy	–	–
KDex62	M/31	c.796C>T	p.Arg266*	NA	c.796C>T	p.Arg266*	NA	1 week	Knees	+
KDex72	F/5	c.796C>T	p.Arg266*	Paternal	c.796C>T	p.Arg266*	Maternal	At birth	Knees and elbows	+
KDex79	M/31	c.796C>T	p.Arg266*	NA	c.796C>T	p.Arg266*	NA	At birth	Knees and elbows	+
KDex90	M/14	c.796C>T	p.Arg266*	Paternal	c.796C>T	p.Arg266*	Maternal	9-10 years	Knees and elbows	+
Compound Heterozygous Mutations										
KDex8[a]	M/38	c.796C>T	p.Arg266*	Maternal	c.218_219del2ins12	p.Gln73Leufs*17[b]	Paternal	At birth	Knees and elbows	+
KDex59	F/16	c.796C>T	p.Arg266*	Paternal	c.218_219del2ins12	p.Gln73Leufs*17[b]	Maternal	At birth	–	+
KDex60	F/30	c.796C>T	p.Arg266*	Paternal	c.218_219del2ins12	p.Gln73Leufs*17[b]	Maternal	At birth	Knees	+
KDex64	F/28	c.796C>T	p.Arg266*	Paternal	c.218_219del2ins12	p.Gln73Leufs*17[b]	Maternal	2 years	–	+
KDex66	F/64	c.796C>T	p.Arg266*	NA	c.218_219del2ins12	p.Gln73Leufs*17[b]	NA	Early infancy	–	–
KDex14[a]	M/20	c.796C>T	p.Arg266*	Maternal	c.455-1G>A	p.Gly152Valfs*21[b]	Paternal	At birth	Knees and elbows	+
KDex58	M/51	c.796C>T	p.Arg266*	NA	c.455-1G>A	p.Gly152Valfs*21[b]	NA	5–6 years	Knees and elbows	+

Abbreviations: M, male; F, Female; NA, not available; c.218_219del2ins12, c.218_219delAGinsTAAACTTTACCT.
[a]Whole-exome sequencing performed.
[b]Predicted from genomic sequences.

Table 2. Major Clinical Differentiating Points among Diffuse Hereditary Palmoplantar Keratoses without Associated Features

Types	Vörner[37]	Unna-Thost[38,39]	Greither[40]	Sybert[41]	Bothnian[31]	Mal de Meleda[8]	Nagashima[2,3]	Gamborg Nielsen[9,10]	Acral Keratoderma[11]
Other names	Diffuse Epidermolytic PPK	Diffuse Nonepidermolytic PPK	Progressive PPK			Keratosis Palmoplantaris Transgradiens of Siemens			
MIM number	144200	600962	144200		600231	248300		244850	
Mode of inheritance	AD	AD	AD	AD	AD	AR	AR	AR	AR
Responsible gene	*KRT1*,[42] *KRT9*[43,44]	*KRT1*[45]	*KRT1*[46]	Unknown	*AQP5*[32,33]	*SLURP1*[12]	*SERPINB7*[a]	Unknown	Unknown
Prevalence rate	4.4/100,000 populations in Northern Ireland[47]	Clinical entity in doubt[1,48,49]	Rare	Rare	Rare	Relatively common in the island of Meleda. 1/100,000 in general populations[50]	1.2/10,000 in Japan[a], 3.1/10,000 in China[a]	Rare	Rare
Age of onset	Within the first year of life	Within the first 2 years of life	Ages 8 to 10	Within the first year of life	During childhood, not as early as during the first year of life	Early infancy	Mostly within the first year of life		
Pathologic findings	Epidermolytic hyperkeratosis	Nonepidermolytic	Nonepidermolytic	Nonepidermolytic	Nonepidermolytic	Nonepidermolytic	Nonepidermolytic	Nonepidermolytic	Nonepidermolytic
Hyperkeratosis	Thick	Thick	Thick	Thick	Mild to thick	Severe	Mild	Thick	Thick
Transgrediens	–	–	+	+	+	+	+	+ (1 of 4)	+
Hyperhidrosis	–	–	+	Not described	+	+	+	Not described	Not described
Whitish change upon water exposure	–	–	–	–	+	–	+	–	–
Development on other areas	–	–	Elbows, knees, flexural areas, and Achilles tendon	Natal cleft, groin, elbows, knees, posterior aspects of forearms, and anterior aspects of legs	–	Knees and elbows, perioral erythema, and periorbital erythema	Knees, elbows, and Achilles tendon area	Only knuckle pads on the dorsa of the fingers	Knees, elbows, ankles, Achilles tendon area
Constricting bands	–	–	+	+	–	+	–	+	+
Spontaneous amputation	–	–	+	+	–	Occasionally	–	Not described	+
Flexion contractures	–	–	–	–	–	+	–	–	–

Abbreviations: AD, autosomal dominant inheritance; AR, autosomal recessive inheritance.
[a]This study.

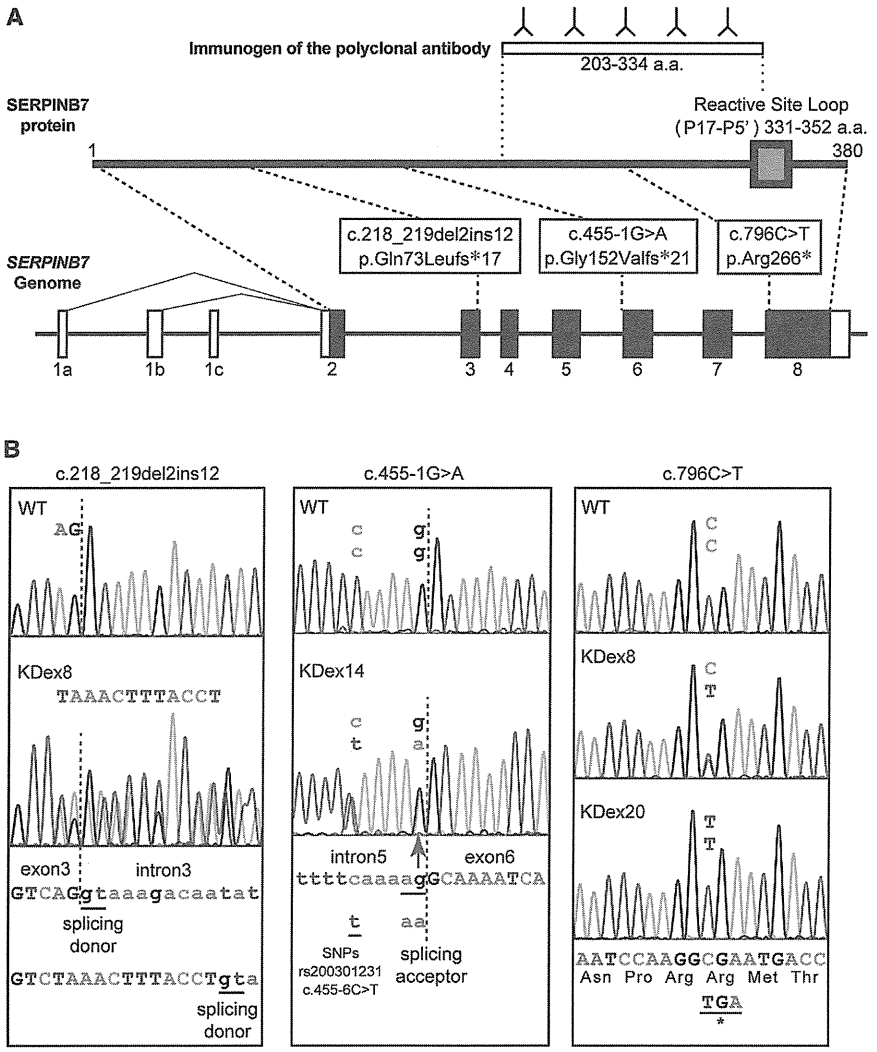

Figure 2. Genomic Organization of *SERPINB7*, Reactive Site Loop for Protease Inhibitory Activity of the SERPINB7 Protein, and Location of NPPK-Causing Mutations

(A) Schematic presentation of the genomic structure of *SERPINB7* (lower) and its encoded protein (middle), SERPINB7. The gray box indicates the reactive site loop indispensable for protease inhibitory activity of SERPINB7. Open and filled boxes indicate exons of untranslated regions and coding regions, respectively. The positions of *SERPINB7* mutations identified in this study are indicated. The immunogen of the anti-SERPINB7 polyclonal antibody is shown at the top.

(B) Heterozygous or homozygous mutated sequences of affected individuals (KDex8, KDex14, and KDex20) compared with the corresponding wild-type sequences. The base and amino acid sequences are shown. The intron-exon junctions are shown with red dotted lines. Intron and exon sequences are shown in lower case and upper case, respectively.

Abbreviations are as follows: c.218_219 del2ins12, c.218_219delAGinsTAAACTTT ACCT.

prevalence rate of NPPK in non-Asian populations was ~0.5/100,000,000. These results well explain why NPPK is so common in PPKs in Japanese populations but has not been reported from non-Asian countries.

Serpins were originally identified as serine protease inhibitors. Serpin molecules are evolutionarily old because even bacteria and Archaea possess them.[15–17] Most serpins identified to date possess protease inhibitory activity, although their protease targets are now known not to be restricted to serine proteases.[16,17] Serpins form covalent complexes with target proteases to inhibit protease activity irreversibly. Human serpins have been divided into nine clades (A–I) by phylogenetic analyses.[15,18] Several congenital diseases have been reported to be caused by deficiencies in the protease inhibitory function of serpins—for example, plasminogen activator inhibitor-1 deficiency (MIM 613329) with mutations in *SERPINE1* (MIM 173360)[19]—or to be caused by polymerization and accumulation of mutated serpins, for example, familial encephalopathy with neuroserpin inclusion bodies (MIM 604218) with mutations in *SERPINI1* (MIM 602445).[20]

SERPINB7 is located on chromosome 18q21.3, forming a cluster of clade-B serpin genes.[18] Clade-B serpins are intracellular serpins, possibly protecting cells from exogenous and endogenous protease-mediated injury.[18] The protease-inhibitory activity of serpins is dependent on the reactive site loop to form a covalent bond with target proteases.[16] The center of the reactive site loop (P1–P1′) is located at amino acids 347–348 of SERPINB7,[16] and the entire region of the reactive site loop (P17–P5′, corresponding to the amino acid region 331–352 of SERPINB7) is predicted to be absent in all of the mutant proteins (Figure 2A). Thus, all of the mutations identified in this study presumably result in a complete loss of the protease inhibitory activity of SERPINB7.

SERPINB7 was originally described as being expressed in kidney mesangial cells and was named *MEGSIN*.[21] However, no renal manifestation has been identified in NPPK individuals. A recent report using a bacterial artificial chromosome transgene expressing Cre in mice under the control of *Serpinb7* regulatory elements showed specific expression of Cre in cornified stratified epithelial cells, but not in kidney mesangial cells,[22] suggesting that *Serpinb7* might be specifically expressed in epidermal keratinocytes in mice. Thus, we next analyzed the expression of *SERPINB7* in human skin. We used a commercial polyclonal antibody (HPA024200; Sigma-Aldrich) raised against a peptide corresponding to the amino acid 203–334 region of human SERPINB7 (Figure 2A). To characterize

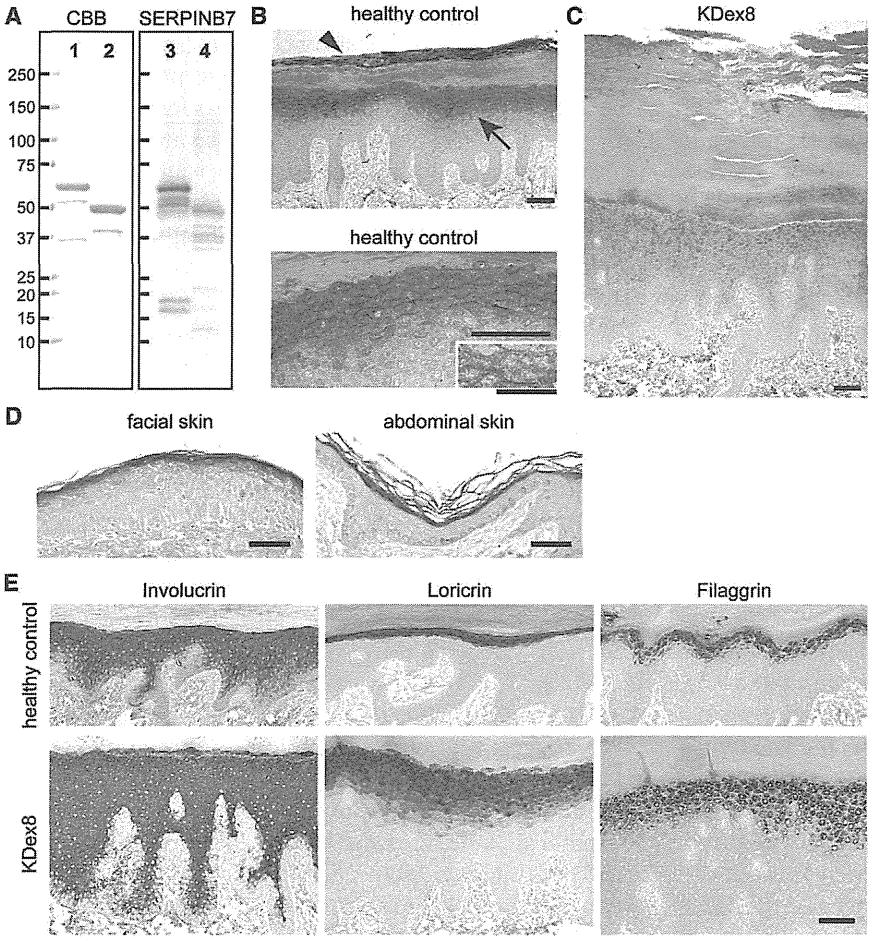

Figure 3. SERPINB7 Localization in the Epidermis and Immunohistochemical Analysis of the Affected Skin

(A) Investigation of the anti-SERPINB7 antibody. GST-fused recombinant full-length human SERPINB7 (lanes 1 and 3) and GST-fused recombinant p.Arg266* mutant (lanes 2 and 4) were analyzed by electrophoresis with Coomassie Brilliant Blue staining (lanes 1 and 2) or with immunoblotting with the anti-SERPINB7 rabbit polyclonal antibody (lanes 3 and 4). Scale bars indicate molecular weights (kDa).

(B) Immunohistochemistry of SERPINB7 in plantar skin of a healthy control. Upper panel shows SERPINB7 in the stratum granulosum (arrow) and in the upper part of the stratum corneum (arrowhead). Lower panel shows the intracellular distribution of SERPINB7 in the stratum granulosum. Scale bars represent 100 μm. Inset in the lower panel shows stratum granulosum cells and intercellular spaces at higher magnification (scale bar represents 50 μm).

(C) Immunohistochemistry of SERPINB7 in the hyperkeratotic plantar skin of NPPK individual of KDex8. Scale bar represents 100 μm.

(D) Immunohistochemistry of SERPINB7 in facial and abdominal skin sections of a healthy control. Scale bars represent 100 μm.

(E) Immunohistochemistry of epidermal differentiation-related proteins in plantar skin of a healthy control (upper panels) and a NPPK individual (KDex8; lower panels). Scale bar represents 100 μm.

the antibody, we performed immunoblotting against GST-fused full-length human SERPINB7 and GST-fused p.Arg266* mutant that were produced in *Escherichia coli* BL21(DE3) by using the pGEX 5X-1 vector (GE Healthcare) in inclusion bodies and purified by washing with 1% Triton X-100 and 4 M urea. The purified proteins showed molecular weights of ~62 kDa and ~50 kDa in SDS-PAGE analysis, respectively (Figure 3A). In immunoblotting analysis, the anti-SERPINB7 antibody recognized both the GST-fused full-length SERPINB7 and GST-fused p.Arg266* mutant (Figure 3A). The immunosignals for the full-length SERPINB7 were stronger than those for the truncated p.Arg266* mutant, suggesting that this polyclonal antibody includes antibodies against peptides corresponding to both the amino acid 203–265 region and the 266–334 region of human SERPINB7 (Figure 2A).

Using this antibody, we performed an immunohistochemical analysis of paraffin wax-embedded sections of healthy human skin and NPPK skin, with antigen retrieval with 15 min boiling in a microwave oven in 100 mM Tris-HCl and 1 mM EDTA buffer (pH 9.0), immunosignal detection with ImmPRESS kit and NovaRed substrates (Vector Laboratories), and counterstaining with methyl green (Wako Pure Chemical). The immunosignals of the antibody were specifically detected from the stratum granulosum and from the upper part of the SC in healthy control plantar skin (Figure 3B). No signal was detected from the lower part of the SC, probably because the tightly packed intracorneocyte proteinaceous structure prevents access of the antibody to the antigen. When the stratum granulosum was observed at higher magnification, signals were observed in the cytoplasm, with a mild concentration to the apical side of the stratum granulosum cells (Figure 3B). In NPPK individuals, the immunosignals of the stratum granulosum and the SC were markedly diminished (KDex8, a compound heterozygote of the c.796C>T and c.218_219del2ins12 mutations; Figure 3C. For other affected individuals, data are not shown or skin biopsies were not performed). Thus, the immunosignals observed in healthy control plantar skin were considered to represent the distribution of SERPINB7. Some nuclear staining was observed in both the healthy control skin and the NPPK skin, which was considered to be nonspecific background (Figures 3B and 3C). Weak cytoplasmic immunosignals were observed in the NPPK skin, which were considered to be due to the p.Arg266* mutant of SERPINB7 or nonspecific background (Figure 3C).

To clarify whether *SERPINB7* expression was limited to the palmoplantar area of the skin, we immunostained facial and abdominal skin sections of healthy controls. SERPINB7 immunosignals were specifically detected from the stratum granulosum and the SC in facial and abdominal epidermis

(Figure 3D), suggesting that *SERPINB7* is expressed in the epidermis of the whole body.

Next, we investigated whether loss of functional SERPINB7 affected epidermal differentiation by using NPPK skin. In NPPK plantar skin, hematoxylin and eosin staining showed acanthosis and orthohyperkeratosis (Figure 1C), as described previously.[3] The localization of epidermal differentiation markers, loricrin, involucrin, and filaggrin, which were detected with anti-loricrin (ab24722; Abcam), anti-involucrin (clone SY5; Sigma Aldrich), and anti-filaggrin (clone FLG01; Thermo Scientific) antibodies, respectively, showed no major keratinocyte differentiation defect in NPPK skin (Figure 3E). Transmission electron microscopic studies of NPPK skin failed to show any major defect in the stratum granulosum or the SC (data not shown).

Loss of functional SERPINB7 might induce overactivation of target proteases in the stratum granulosum and the SC. Because no apparent change was observed in the stratum granulosum except for thickening, we reinvestigated the skin phenotype of NPPK, looking especially for any finding of changes in the SC. We found that the NPPK skin showed a whitish spongy appearance within 10 min of water exposure specifically in the reddish hyperkeratotic area (Figure 4A). The wrinkling of palms that is observed after water exposure in cystic fibrosis (MIM 219700)[23,24] was not apparent, even after 30 min of water exposure (Figure 4A). These phenotypes suggested enhanced water permeation into the surface of the SC in NPPK lesional skin.

Thus, we next performed a transepidermal water loss (TEWL) analysis prior to and after water exposure in three NPPK individuals and three healthy controls. TEWL was measured at the lesional and nonlesional skin of dorsal hands and inner wrists in each NPPK individual and at the corresponding skin area in each healthy control with a Vapo Scan AS-VT100RS (Asahi Biomed) at room temperature (20°C–22°C) and 40%–60% humidity to avoid the effects of hyperhidrosis. The mean TEWL value was calculated from measurements of at least eight different points under each skin condition. Before water exposure, the mean TEWL values were higher in the lesional skin of NPPK individuals than in the nonlesional skin of NPPK individuals or the corresponding skin area of normal healthy controls (Figure 4B), when analyzed by using the Tukey-Kramer multiple-comparisons test with the Prism software (ver. 6; GraphPad Software). Next, the hands of NPPK individuals and healthy controls were immersed in water at 37°C for 30 min. After water exposure, TEWL values were significantly elevated in all skin conditions in all NPPK skin and in all healthy control skin (data not shown), and the mean TEWL values were significantly elevated on water exposure in any skin condition (Figure 4B) when analyzed with Student's t test with the Prism software.

After water exposure, the mean TEWL values were higher in the lesional skin of NPPK individuals than in the nonlesional skin of NPPK individuals or the corresponding skin areas of healthy controls (Figure 4B) when analyzed with the Tukey–Kramer multiple-comparisons test. Because the TEWL instrument measures water evaporation from the skin surface, the TEWL values after water exposure might correspond mostly to water evaporation from water-swollen SC. Thus, these results suggest that water permeation into the SC is specifically facilitated in NPPK lesional skin.

Here, we identified that loss-of-function mutations in *SERPINB7* cause NPPK and established NPPK genetically as a distinct clinical entity within hereditary diffuse PPKs without associated features. While *SERPINB7* was considered to be expressed in the epidermis of the whole body, the affected skin area of NPPK is limited to hands, feet, knees, and elbows, the reason for which remains unknown. Such limitations in the affected skin area with a deficiency of gene products that are ubiquitously expressed in the epidermis have been observed in several other types of PPK: Vohwinkel syndrome (MIM 124500), caused by mutations in *GJB2* (MIM 121011),[25] and type I striate PPK (MIM 148700), caused by mutations in *DSG1* (MIM 125670).[26] The effects on the knees and elbows in NPPK suggest that chronic exposure to mechanical stress might have a role in the development of NPPK skin lesions, and the lesions in NPPK are limited to chronic mechanical stress-exposed areas of the skin. Thus, SERPINB7 might inhibit mechanical stress-induced proteases and protect keratinocytes or corneocytes from protease-mediated cellular damage.

Our findings suggest that NPPK is a genetic dermatosis caused by a deficiency of an intracellular protease inhibitor. Deficiencies of the protease inhibitors, LEKTI, encoded by *SPINK5* (MIM 605010), and cystatin A, encoded by *CSTA* (MIM 184600), have been reported in Netherton syndrome (MIM 256500)[27] and exfoliative ichthyosis (MIM 607936),[28] respectively. In Netherton syndrome, overactivation of secreted extracellular proteases, kallikreins, has been suggested to induce overdesquamation via excessive degradation of cell adhesion molecules in the SC[29] and skin inflammatory responses through thymic stromal lymphopoietin expression, mediated by unregulated activation of protease-activated receptor-2.[30] In exfoliative ichthyosis, defects in desmosome-mediated cell-cell adhesion in the lower levels of the epidermis have been suggested to cause coarse peeling of skin on the palms and soles.[28] However, the precise pathophysiology or protease overactivation induced by the loss of cystatin A has not yet been characterized.

As corneocytes lose the cell membrane on cornification, it is unclear whether SERPINB7 is held within corneocytes at the SC. But the phenotype of NPPK differs completely from that of Netherton syndrome because desquamation is rather prolonged in the erythematous hyperkeratotic area in NPPK, suggesting that the target proteases of SERPINB7 are unlikely to be associated with the desquamation process. Here, we observed a whitish spongy change

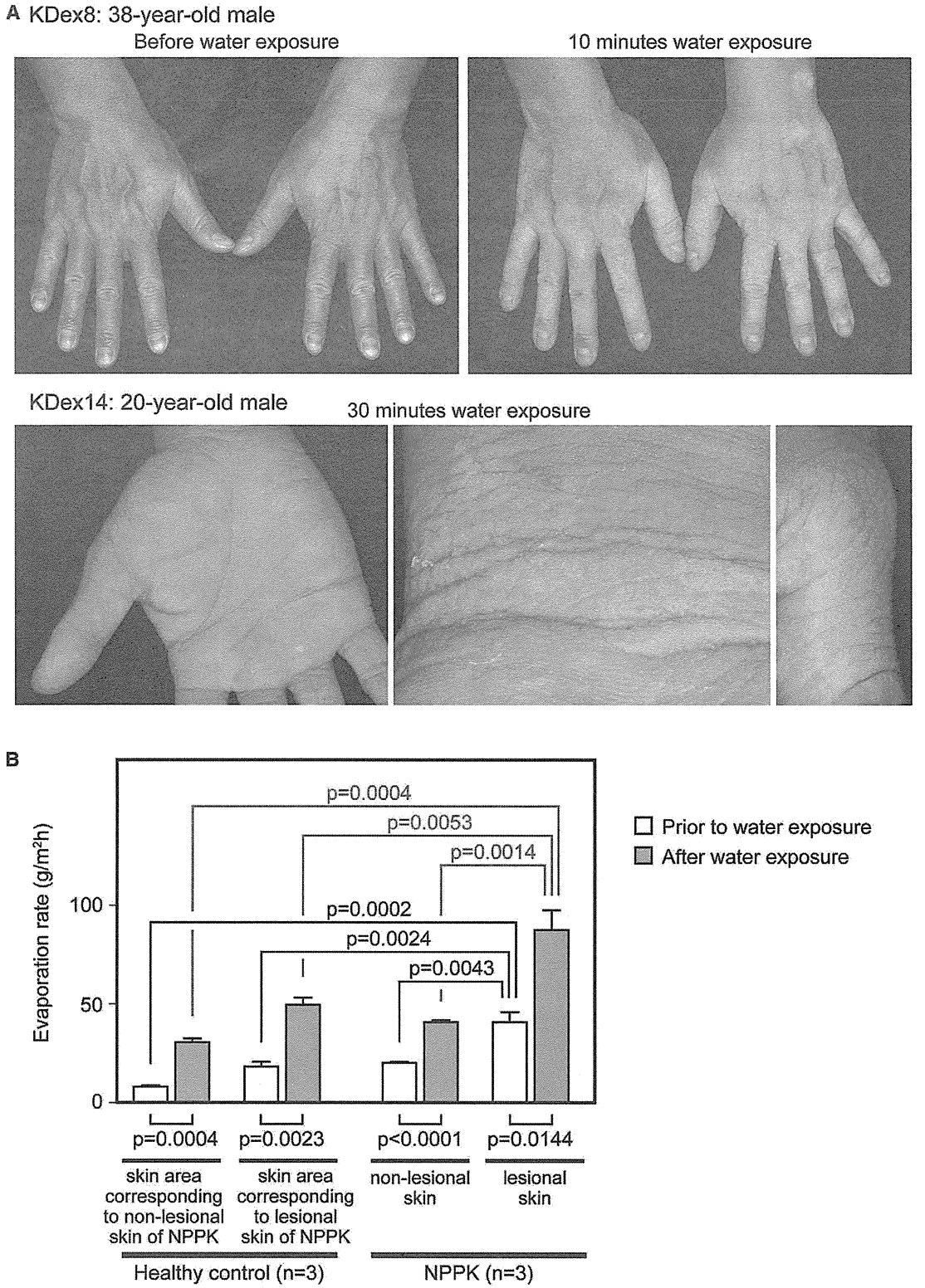

Figure 4. Changes upon Water Exposure in NPPK Lesional Skin

(A) Clinical phenotype of the hands of the proband (KDex8) prior to water exposure (upper left panel) and after 10 min water exposure (upper right panel), and the clinical phenotype of the hands of the proband (KDex14) after 30 min water exposure: the palm (lower left panel), inner wrist (lower middle panel), and dorsa of the thumb (lower right panel).

(B) Means of TEWL values prior to water exposure and after 30 min of water exposure in the lesional skin and nonlesional skin of NPPK individuals (n = 3; KDex8, KDex14, and KDex79) and in the corresponding skin area of healthy controls (n = 3). In each skin condition, the means of TEWL were compared upon water exposure (lower lines). The means of TEWL were compared between lesional and nonlesional skin of NPPK individuals and the corresponding skin area of healthy controls before water exposure (upper black lines) and after water exposure (upper red lines).

in the SC on exposure to water in the lesional skin of NPPK. This change is caused by a loss of integrity in the SC structure, probably due to overactivation of target proteases of SERPINB7. Such a whitish change in the skin upon water exposure has been reported in an autosomal-dominant Bothnian-type PPK (MIM 600231) with mutations in *AQP5* (MIM 600442),[31–33] and in the aquagenic keratoderma associated with cystic fibrosis with mutations in *CFTR* (MIM 602421),[23,24] but the pathophysiology of the whitish changes might differ among these diseases.

Together with the strong immunosignals of SERPINB7 in the SC, we propose that loss of functional SERPINB7 induces overactivation of intracorneocyte proteases specifically in the affected skin area, which induces degradation of the integrated proteinaceous structure of the corneocytes and facilitates water permeation into the SC. Additional functional assays and molecular biological analyses are required to investigate the changes in the water repellant properties of the SC surface in NPPK skin.

Various proteases are present in the stratum granulosum and the SC[34–36]. Additionally, the epidermis is attacked by various exogenous proteases—originating from bacteria, fungi, virus, pollen, and house dust mites—and endogenous proteases, originating from infiltrating cells.[35] Appropriate control of the activity of these proteases by endogenous protease inhibitors is likely important in maintaining skin homeostasis. Our discovery of loss-of-function mutations in *SERPINB7* in NPPK should provide insights into the functions and regulatory mechanisms of proteases and protease inhibitors in the epidermis. Future studies will aim to identify the target proteases of SERPINB7 in the steady state and in mechanically stressed states. It is also important to understand the pathophysiology of the putative protease overactivation in NPPK skin; that is, how the proteinaceous structure of the SC and integrity of the SC barrier are affected and whether the reddish hyperkeratosis and inflammatory cell infiltrations are secondary changes via augmented external stimuli through protease-mediated damage to the SC or direct effects of intraepidermal overactivation of proteases. The development of specific protease inhibitors mimicking SERPINB7 might allow pathogenesis-based therapies for NPPK.

Supplemental Data

Supplemental Data includes one figure and one table and can be found with this article online at http://www.cell.com/AJHG/home.

Acknowledgments

We thank our clinical colleagues, and family members who contributed the samples used in this study. We also thank Nobuyo Nishimura, Hiromi Sakuragi, Asami Hirakiyama, Kazunari Shibata, and the Collaborative Research Resources of Keio University School of Medicine for technical support. This work was supported in parts by Health and Labour Sciences Research Grants for Research on Rare and Intractable Diseases, for Research on Allergic Disease and Immunology, and for Research on Measures for Intractable Diseases from the Ministry of Health, Labour and Welfare of Japan, The Grant of National Center for Child Health and Development (24-5), and Grants-in-Aid for Scientific Research from the Ministry of Education, Culture, Sports, Science and Technology, Japan. This manuscript is dedicated to the memory of Professor Masaji Nagashima. Potential conflict of interest: M.A. has consultancy arrangements with Daiichi Sankyo Co. A.K., A.S., and T.S. have been supported by one or more grants from MSD K.K. and Maruho Co., Ltd. This work was supported in part by a grant from Maruho Co., Ltd.

Received: August 23, 2013
Revised: September 19, 2013
Accepted: September 25, 2013
Published: October 24, 2013

Web Resources

The URLs for data presented here are as follows:

1000 Genomes, http://browser.1000genomes.org
NCBI dbSNPs, http://www.ncbi.nlm.nih.gov/projects/SNP/
NCBI RefSeq, http://www.ncbi.nlm.nih.gov/refseq/
NHLBI Exome Sequencing Project (ESP) Exome Variant Server, http://evs.gs.washington.edu/EVS/
Online Mendelian Inheritance in Man (OMIM), http://www.omim.org/

References

1. Lucker, G.P., Van de Kerkhof, P.C., and Steijlen, P.M. (1994). The hereditary palmoplantar keratoses: an updated review and classification. Br. J. Dermatol. *131*, 1–14.
2. Mitsuhashi, Y., and Hashimato, I. (1989). Keratosis palmoplantaris Nagashima. Dermatologica *179*, 231.
3. Kabashima, K., Sakabe, J., Yamada, Y., and Tokura, Y. (2008). "Nagashima-type" keratosis as a novel entity in the palmoplantar keratoderma category. Arch. Dermatol. *144*, 375–379.
4. Mitsuhashi, Y., Hashimoto, I., and Takahashi, M. (1989). Meleda type keratosis palmoplantaris (Nagashima). Practical Dermatol. *11*, 297–300, (in Japanese).
5. Nagashima, M. (1977). Palmoplantar keratoses. In Handbook of Human Genetics, *Volume 9*, O. Miura and K. Ochiai, eds. (Tokyo: Igaku Shoin), pp. 23–27, (in Japanese).
6. Isoda, H., Kabashima, K., and Tokura, Y. (2009). 'Nagashima-type' keratosis palmoplantaris in two siblings. J. Eur. Acad. Dermatol. Venereol. *23*, 737–738.
7. Sakabe, J., Kabashima, K., Sugita, K., and Tokura, Y. (2009). Possible involvement of T lymphocytes in the pathogenesis of Nagashima-type keratosis palmoplantaris. Clin. Exp. Dermatol. *34*, e282–e284.
8. Hovorka, O., and Ehlers, E. (1897). Mal de Meleda. Arch. Dermatol. Res. *40*, 251–256.
9. Gamborg Nielsen, P. (1985). Two different clinical and genetic forms of hereditary palmoplantar keratoderma in the northernmost county of Sweden. Clin. Genet. *28*, 361–366.
10. Kastl, I., Anton-Lamprecht, I., and Gamborg Nielsen, P. (1990). Hereditary palmoplantar keratosis of the Gamborg Nielsen type. Clinical and ultrastructural characteristics of a new type of autosomal recessive palmoplantar keratosis. Arch. Dermatol. Res. *282*, 363–370.

11. Nesbitt, L.T., Jr., Rothschild, H., Ichinose, H., Stein, W., 3rd, and Levy, L. (1975). Acral keratoderma. Arch. Dermatol. *111*, 763–768.
12. Fischer, J., Bouadjar, B., Heilig, R., Huber, M., Lefèvre, C., Jobard, F., Macari, F., Bakija-Konsuo, A., Ait-Belkacem, F., Weissenbach, J., et al. (2001). Mutations in the gene encoding SLURP-1 in Mal de Meleda. Hum. Mol. Genet. *10*, 875–880.
13. Sasaki, T., Niizeki, H., Shimizu, A., Shiohama, A., Hirakiyama, A., Okuyama, T., Seki, A., Kabashima, K., Otsuka, A., Ishiko, A., et al. (2012). Identification of mutations in the prostaglandin transporter gene SLCO2A1 and its phenotype-genotype correlation in Japanese patients with pachydermoperiostosis. J. Dermatol. Sci. *68*, 36–44.
14. The 1000 Genomes Project Consortium. (2012). An integrated map of genetic variation from 1,092 human genomes. Nature *491*, 56–65.
15. Irving, J.A., Pike, R.N., Lesk, A.M., and Whisstock, J.C. (2000). Phylogeny of the serpin superfamily: implications of patterns of amino acid conservation for structure and function. Genome Res. *10*, 1845–1864.
16. Gettins, P.G.W. (2002). Serpin structure, mechanism, and function. Chem. Rev. *102*, 4751–4804.
17. Law, R.H.P., Zhang, Q., McGowan, S., Buckle, A.M., Silverman, G.A., Wong, W., Rosado, C.J., Langendorf, C.G., Pike, R.N., Bird, P.I., and Whisstock, J.C. (2006). An overview of the serpin superfamily. Genome Biol. *7*, 216.
18. Silverman, G.A., Whisstock, J.C., Askew, D.J., Pak, S.C., Luke, C.J., Cataltepe, S., Irving, J.A., and Bird, P.I. (2004). Human clade B serpins (ov-serpins) belong to a cohort of evolutionarily dispersed intracellular proteinase inhibitor clades that protect cells from promiscuous proteolysis. Cell. Mol. Life Sci. *61*, 301–325.
19. Fay, W.P., Shapiro, A.D., Shih, J.L., Schleef, R.R., and Ginsburg, D. (1992). Brief report: complete deficiency of plasminogen-activator inhibitor type 1 due to a frame-shift mutation. N. Engl. J. Med. *327*, 1729–1733.
20. Davis, R.L., Shrimpton, A.E., Carrell, R.W., Lomas, D.A., Gerhard, L., Baumann, B., Lawrence, D.A., Yepes, M., Kim, T.S., Ghetti, B., et al. (2002). Association between conformational mutations in neuroserpin and onset and severity of dementia. Lancet *359*, 2242–2247.
21. Miyata, T., Nangaku, M., Suzuki, D., Inagi, R., Uragami, K., Sakai, H., Okubo, K., and Kurokawa, K. (1998). A mesangium-predominant gene, megsin, is a new serpin upregulated in IgA nephropathy. J. Clin. Invest. *102*, 828–836.
22. Wang, Y., Guo, Q., Casey, A., Lin, C., and Chen, F. (2012). A new tool for conditional gene manipulation in a subset of keratin-expressing epithelia. Genesis *50*, 899–907.
23. Garçon-Michel, N., Roguedas-Contios, A.-M., Rault, G., Le Bihan, J., Ramel, S., Revert, K., Dirou, A., and Misery, L. (2010). Frequency of aquagenic palmoplantar keratoderma in cystic fibrosis: a new sign of cystic fibrosis? Br. J. Dermatol. *163*, 162–166.
24. Weibel, L., and Spinas, R. (2012). Images in clinical medicine. Aquagenic wrinkling of palms in cystic fibrosis. N. Engl. J. Med. *366*, e32.
25. Maestrini, E., Korge, B.P., Ocaña-Sierra, J., Calzolari, E., Cambiaghi, S., Scudder, P.M., Hovnanian, A., Monaco, A.P., and Munro, C.S. (1999). A missense mutation in connexin26, D66H, causes mutilating keratoderma with sensorineural deafness (Vohwinkel's syndrome) in three unrelated families. Hum. Mol. Genet. *8*, 1237–1243.
26. Rickman, L., Simrak, D., Stevens, H.P., Hunt, D.M., King, I.A., Bryant, S.P., Eady, R.A., Leigh, I.M., Arnemann, J., Magee, A.I., et al. (1999). N-terminal deletion in a desmosomal cadherin causes the autosomal dominant skin disease striate palmoplantar keratoderma. Hum. Mol. Genet. *8*, 971–976.
27. Chavanas, S., Bodemer, C., Rochat, A., Hamel-Teillac, D., Ali, M., Irvine, A.D., Bonafé, J.L., Wilkinson, J., Taïeb, A., Barrandon, Y., et al. (2000). Mutations in SPINK5, encoding a serine protease inhibitor, cause Netherton syndrome. Nat. Genet. *25*, 141–142.
28. Blaydon, D.C., Nitoiu, D., Eckl, K.-M., Cabral, R.M., Bland, P., Hausser, I., van Heel, D.A., Rajpopat, S., Fischer, J., Oji, V., et al. (2011). Mutations in CSTA, encoding Cystatin A, underlie exfoliative ichthyosis and reveal a role for this protease inhibitor in cell-cell adhesion. Am. J. Hum. Genet. *89*, 564–571.
29. Descargues, P., Deraison, C., Bonnart, C., Kreft, M., Kishibe, M., Ishida-Yamamoto, A., Elias, P., Barrandon, Y., Zambruno, G., Sonnenberg, A., and Hovnanian, A. (2005). Spink5-deficient mice mimic Netherton syndrome through degradation of desmoglein 1 by epidermal protease hyperactivity. Nat. Genet. *37*, 56–65.
30. Briot, A., Deraison, C., Lacroix, M., Bonnart, C., Robin, A., Besson, C., Dubus, P., and Hovnanian, A. (2009). Kallikrein 5 induces atopic dermatitis-like lesions through PAR2-mediated thymic stromal lymphopoietin expression in Netherton syndrome. J. Exp. Med. *206*, 1135–1147.
31. Lind, L., Lundström, A., Hofer, P.A., and Holmgren, G. (1994). The gene for diffuse palmoplantar keratoderma of the type found in northern Sweden is localized to chromosome 12q11-q13. Hum. Mol. Genet. *3*, 1789–1793.
32. Blaydon, D.C., Lind, L.K., Plagnol, V., Linton, K.J., Smith, F.J.D., Wilson, N.J., McLean, W.H.I., Munro, C.S., South, A.P., Leigh, I.M., et al. (2013). Mutations in AQP5, Encoding a Water-Channel Protein, Cause Autosomal-Dominant Diffuse Nonepidermolytic Palmoplantar Keratoderma. Am. J. Hum. Genet. *93*, 330–335.
33. Cao, X., Yin, J., Wang, H., Zhao, J., Zhang, J., Dai, L., Zhang, J., Jiang, H., Lin, Z., and Yang, Y. (2013). Mutation in AQP5, Encoding Aquaporin 5, Causes Palmoplantar Keratoderma Bothnia Type. J. Invest. Dermatol., in press.
34. Kamata, Y., Taniguchi, A., Yamamoto, M., Nomura, J., Ishihara, K., Takahara, H., Hibino, T., and Takeda, A. (2009). Neutral cysteine protease bleomycin hydrolase is essential for the breakdown of deiminated filaggrin into amino acids. J. Biol. Chem. *284*, 12829–12836.
35. Meyer-Hoffert, U. (2009). Reddish, scaly, and itchy: how proteases and their inhibitors contribute to inflammatory skin diseases. Arch. Immunol. Ther. Exp. (Warsz.) *57*, 345–354.
36. Matsui, T., Miyamoto, K., Kubo, A., Kawasaki, H., Ebihara, T., Hata, K., Tanahashi, S., Ichinose, S., Imoto, I., Inazawa, J., et al. (2011). SASPase regulates stratum corneum hydration through profilaggrin-to-filaggrin processing. EMBO Mol Med *3*, 320–333.
37. Vörner, H. (1901). Zur Kenntnis des Keratoma hereditarium palmare et plantare. Arch. Dermatol. Syph. *56*, 3–31.
38. Thost A. (1880). Über erbliche ichthyosis palmaris et plantaris cornea. (Med. Diss). Horning J., ed. Heidelberg.
39. Unna, P. (1883). Über das Keratoma palmare et plantare hereditarium, eine Studie zur Kerato-Nosologie. Arch. Dermatol. Syph. *15*, 231–270.
40. Greither, A. (1952). Keratosis extremitatum hereditaria progrediens mit dominantem Erbgang. Hautarzt *3*, 198–203.